A Review on the Numerical Solution of the 1D Euler Equations

Hudson, Justin

2006

MIMS EPrint: **2006.9**

Manchester Institute for Mathematical Sciences
School of Mathematics

The University of Manchester

ISSN 1749-9097

A Review on the Numerical Solution of the 1D Euler Equations

Justin Hudson *

Abstract

This paper presents a review on the numerical solution of the Euler equations. Three different high resolution versions of the following schemes are considered: Roe's scheme, the HLLE scheme and the AUSM+ scheme. We present a variety of test cases, each designed to test the robustness of each scheme and compare the results to determine which scheme was the most accurate.

1 Introduction

The numerical solution of the Euler equations has been thoroughly researched with numerous papers published on the subject, e.g. Roe [10], Liou [9], Jiang & Shu [6], Yee [16] and Einfeldt *et al.* [1]. The Euler equations have been a standard test model for the derivation of numerous schemes in order to test their accuracy. This is due to a variety of analytical solutions being obtainable and the full system is homogeneous.

In this paper, we present a brief review of three different numerical schemes and their accuracy when used to approximate the Euler equations for a variety of test problems. We are particularly interested in high resolution schemes and adapt versions of Roe's scheme [10], the HLLE scheme [1, 2] and the AUSM+ scheme [9, 8]. Four different test cases are considered to test numerous potential flaws of the schemes and the results compared to an analytical solution (if it exists) to determine the accuracy of the schemes.

*School of Mathematics, University of Manchester, Sackville Street, Manchester, M60 1QD (`justin.hudson@manchester.ac.uk`)

We are particularly interested in how robust the schemes are in terms of accuracy and the maximum CFL number required to minimise numerical oscillations (for computational efficiency).

In the next Section, we briefly introduce the Euler equations with the schemes discretised for the equations in Section 3. We then present four different test cases and the numerical results in Section 4 with a conclusion being presented in Section 5.

2 Euler Equations

We now present a brief discussion on the Euler equations in 1D, but refer the reader to LeVeque [7] and Toro [12] for a more detailed discussion (and derivation). The Euler equations governing the flow of a compressible gas in 1D comprise

$$\begin{bmatrix} \rho \\ \rho u \\ E \end{bmatrix}_t + \begin{bmatrix} \rho u \\ \rho u^2 + p \\ u(E+p) \end{bmatrix}_x = 0, \tag{2.1}$$

where ρ is the density, u is the particle velocity, p is pressure and the total energy per unit volume is

$$E = \left(e + \frac{1}{2}u^2\right)\rho.$$

Here e is the specific internal energy, which for ideal gases is

$$e = \frac{p}{(\gamma-1)\rho} \quad \Rightarrow \quad p = (\gamma-1)(E - \frac{1}{2}\rho u^2), \tag{2.2}$$

where γ denotes the ratio of specific heat capacities of the gas.

The Jacobian matrix of the system (2.1) for ideal gases (2.2) is

$$\mathbf{A} = \begin{bmatrix} 0 & 1 & 0 \\ \frac{1}{2}(\gamma-3)u^2 & (3-\gamma)u & \gamma-1 \\ u\left(\frac{1}{2}(\gamma-1)u^2 - H\right) & H-(\gamma-1)u^2 & \gamma u \end{bmatrix},$$

where the total specific enthalpy is

$$H = \frac{E+p}{\rho} = \frac{a^2}{\gamma-1} + \frac{1}{2}u^2$$

and the sound speed is

$$a = \sqrt{\frac{\gamma p}{\rho}} = \sqrt{\frac{\gamma}{\rho}(\gamma - 1)(E - \frac{1}{2}\rho u^2)}.$$

The eigenvalues of $\mathbf{A}$ are

$$\lambda_1 = u - a, \quad \lambda_2 = u \quad \text{and} \quad \lambda_3 = u + a,$$

whose corresponding eigenvectors are

$$\mathbf{e}_1 = \begin{bmatrix} 1 \\ u - a \\ H - ua \end{bmatrix}, \quad \mathbf{e}_2 = \begin{bmatrix} 1 \\ u \\ \frac{1}{2}u^2 \end{bmatrix} \quad \text{and} \quad \mathbf{e}_3 = \begin{bmatrix} 1 \\ u + a \\ H + ua \end{bmatrix}.$$

3 High Resolution Schemes

To obtain a numerical approximation of the Euler equations (2.1), we use three different numerical schemes to determine which is the most accurate. All three schemes are high resolution schemes, i.e. they are second order accurate away from shocks and satisfy the Total Variational Diminishing (TVD) property. The first scheme is based on Roe's scheme [10] and was discussed by Hubbard & Garcia-Navarro [4], the second scheme is the HLLE scheme [1], which is an adapted version of the HLL scheme [2], and the third scheme is the AUSM+ scheme as discussed by Liou [9].

The Euler equations are a system of homogeneous conservation laws,

$$\mathbf{w}_t + \mathbf{F}(\mathbf{w})_x = 0, \tag{3.1}$$

where $\mathbf{F}(\mathbf{w})$ is the flux-function. To obtain a conservative approximation of homogeneous systems of conservation laws, we only consider numerical schemes of the form

$$\mathbf{w}_i^{n+1} = \mathbf{w}_i^n - s(\mathbf{F}^*_{i+\frac{1}{2}} - \mathbf{F}^*_{i-\frac{1}{2}}), \tag{3.2}$$

where $s = \frac{\Delta t}{\Delta x}$, Δx and Δt are the step sizes in space and time respectively, $\mathbf{F}^*_{i+\frac{1}{2}}$ is the numerical flux and

$$\mathbf{w}_i^n \approx \frac{1}{\Delta x}\int_{x_{i-\frac{1}{2}}}^{x_{i+\frac{1}{2}}} \mathbf{w}(x, t^n)\ dx$$

is the numerical approximation.

To ensure the schemes remains stable, the time step is calculated using

$$\Delta t = \frac{\nu \Delta x}{\max(|\lambda|)},$$

where $\max(|\lambda|)$ is the maximum wave speed and $\nu \leq 1$ is the required Courant (CFL) number.

We now present a discussion and discretisation of the three schemes.

3.1 Roe's Scheme

Hubbard & Garcia-Navarro [4] discussed an adapted form of Roe's scheme [10], which is a high resolution scheme. The numerical flux-function is

$$\mathbf{F}^*_{i+\frac{1}{2}} = \frac{1}{2}(\mathbf{F}^n_{i+1} + \mathbf{F}^n_i) - \frac{1}{2}\sum_{k=1}^{p}\left[\tilde{\alpha}_k|\tilde{\lambda}_k|(1 - \Phi(\theta_k)(1 - |\nu_k|))\tilde{\mathbf{e}}_k\right]_{i+\frac{1}{2}}$$

where

$$\nu_k = s\tilde{\lambda}_k, \quad \theta_k = \frac{(\tilde{\alpha}_k)_{I+\frac{1}{2}}}{(\tilde{\alpha}_k)_{i+\frac{1}{2}}}, \quad I = i - \operatorname{sgn}(\nu_k)_{i+\frac{1}{2}},$$

and $\Phi(\theta_k)$ is the minmod flux-limiter,

$$\Phi(\theta_k) = \max(0, \min(1, \theta_k)).$$

Here, the $\tilde{}$ is called the Roe average and $\tilde{\lambda}$, $\tilde{\mathbf{e}}$ and $\tilde{\alpha}$ are the eigenvalues, eigenvectors and wave strengths of the Roe averaged Jacobian matrix, $\tilde{\mathbf{A}}$. The Roe averaged eigenvalues, eigenvectors and wave strengths are determined from the Roe decomposition (see [10, 4, 5] for more details)

$$\Delta \mathbf{F} = \sum_{k=1}^{p} \tilde{\alpha}_k \tilde{\lambda}_k \tilde{\mathbf{e}}_k = \tilde{\mathbf{A}}\Delta \mathbf{w},$$

where $\Delta \mathbf{w} = \mathbf{w}_R - \mathbf{w}_L$ and p is the number of components in the system ($p = 3$ for the Euler equations).

For the Euler equations (2.1) with ideal gases (2.2), Toro [12] obtained the following Roe averaged Jacobian matrix,

$$\tilde{\mathbf{A}} = \begin{bmatrix} 0 & 1 & 0 \\ \frac{1}{2}(\gamma-3)\tilde{u}^2 & (3-\gamma)\tilde{u} & \gamma - 1 \\ \tilde{u}\left(\frac{1}{2}(\gamma-1)\tilde{u}^2 - \tilde{H}\right) & \tilde{H} - (\gamma-1)\tilde{u^2} & \gamma\tilde{u} \end{bmatrix},$$

whose eigenvalues are

$$\tilde{\lambda}_1 = \tilde{u} - \tilde{a}, \quad \tilde{\lambda}_2 = \tilde{u} \quad \text{and} \quad \tilde{\lambda}_3 = \tilde{u} + \tilde{a}$$

with corresponding eigenvectors

$$\tilde{\mathbf{e}}_1 = \begin{bmatrix} 1 \\ \tilde{u} - \tilde{a} \\ \tilde{H} - \tilde{u}\tilde{a} \end{bmatrix}, \quad \tilde{\mathbf{e}}_2 = \begin{bmatrix} 1 \\ \tilde{u} \\ \frac{1}{2}\tilde{u}^2 \end{bmatrix} \quad \text{and} \quad \tilde{\mathbf{e}}_3 = \begin{bmatrix} 1 \\ \tilde{u} + \tilde{a} \\ \tilde{H} + \tilde{u}\tilde{a} \end{bmatrix},$$

where the Roe average values are

$$\tilde{u} = \frac{\sqrt{\rho_L}u_L + \sqrt{\rho_R}u_R}{\sqrt{\rho_L} + \sqrt{\rho_R}}, \quad \tilde{H} = \frac{\sqrt{\rho_L}H_L + \sqrt{\rho_R}H_R}{\sqrt{\rho_L} + \sqrt{\rho_R}}$$

and

$$\tilde{a} = \sqrt{(\gamma - 1)(\tilde{H} - \frac{1}{2}\tilde{u}^2)}.$$

Toro also determined the following wave strengths,

$$\tilde{\alpha}_2 = \frac{(\gamma - 1)}{\tilde{a}^2}\left(\left(\tilde{H} - \tilde{u^2}\right)\Delta\rho + \tilde{u}\Delta(\rho u) - \Delta E\right),$$

$$\tilde{\alpha}_1 = \frac{1}{2\tilde{a}}\left(\left(\tilde{u} + \tilde{a}\right)\Delta\rho - \Delta(\rho u) - \tilde{a}\tilde{\alpha}_2\right), \quad \text{and} \quad \tilde{\alpha}_3 = \Delta\rho - (\tilde{\alpha}_1 + \tilde{\alpha}_2).$$

3.2 HLLE

Einfeldt *et al.* [1] discussed an adapted version of the HLL scheme [2] called the HLLE scheme, which can be viewed as a modification of Roe's scheme. In this paper, we adapt the HLLE scheme to a high resolution scheme,

$$\mathbf{F}^*_{i+\frac{1}{2}} = \frac{1}{2}(\mathbf{F}^n_{i+1} + \mathbf{F}^n_i) - \frac{1}{2}\sum_{k=1}^{p}\left[\tilde{\alpha}_k\tilde{Q}_k(1 - \Phi(\theta_k)(1 - s\tilde{Q}_k))\tilde{\mathbf{e}}_k\right]_{i+\frac{1}{2}},$$

where

$$\left(\tilde{Q}_k\right)^n_{i+\frac{1}{2}} = \left[\frac{\left(b^+ + b^-\right)\tilde{\lambda}_k - 2b^+b^-}{b^+ - b^-}\right]^n_{i+\frac{1}{2}},$$

$$b^+_{i+\frac{1}{2}} = \max\left(b^R_{i+\frac{1}{2}}, 0\right), \quad b^-_{i+\frac{1}{2}} = \min\left(b^L_{i+\frac{1}{2}}, 0\right)$$

and the numerical signal velocities for the Euler equations with ideal gases are

$$b^R_{i+\frac{1}{2}} = \max\left(\tilde{u} + \tilde{a}, u^n_{i+1} + a^n_{i+1}\right) \quad \text{and} \quad b^L_{i+\frac{1}{2}} = \min\left(\tilde{u} - \tilde{a}, u^n_i - a^n_i\right).$$

In this paper, we use the Roe average values (in the previous section) to determine $\tilde{\lambda}$, $\tilde{\mathbf{e}}$ and $\tilde{\alpha}$.

3.3 AUSM+

Liou [9] discussed an improved version of the AUSM scheme [8], which re-writes the flux-function, $\mathbf{F}(\mathbf{w})$, as a sum of the convective and pressure terms,

$$\mathbf{F}(\mathbf{w}) = \mathbf{F}^{(c)} + \mathbf{P},$$

where

$$\mathbf{F}^{(c)} = Ma\boldsymbol{\Psi}, \quad \boldsymbol{\Psi} = \begin{bmatrix} \rho \\ \rho u \\ \rho H \end{bmatrix} \quad \text{and} \quad \mathbf{P} = \begin{bmatrix} 0 \\ p \\ 0 \end{bmatrix},$$

and discretises them separately. Here, $M = ua^{-1}$ denotes the Mach number and a the sound speed. One advantage of this scheme is that the Jacobian matrix does not need to be calculated. The numerical flux-function of the AUSM+ scheme is

$$\mathbf{F}^*_{i+\frac{1}{2}} = \frac{1}{2}a^n_{i+\frac{1}{2}}\left(m^n_{i+\frac{1}{2}}\left(\boldsymbol{\Psi}^n_{i+1} + \boldsymbol{\Psi}^n_i\right) - |m^n_{i+\frac{1}{2}}|\left(\boldsymbol{\Psi}^n_{i+1} - \boldsymbol{\Psi}^n_i\right)\right) + \mathbf{P}^n_{i+\frac{1}{2}}, \tag{3.3}$$

where $m^n_{i+\frac{1}{2}}$ is the numerical approximation of the interface mach number,

$$m^n_{i+\frac{1}{2}} = \mathcal{M}^+(M^n_i) + \mathcal{M}^-(M^n_{i+1})$$

with

$$\mathcal{M}^\pm(M) = \begin{cases} \frac{1}{2}(M \pm |M|) & \text{if } |M| \geq 1, \\ \pm\frac{1}{2}(M \pm 1)^2 \pm \beta(M^2 - 1)^2 & \text{otherwise,} \end{cases}$$

and $a^n_{i+\frac{1}{2}}$ is the numerical approximation of the sound speed, which for this paper we take as

$$a^n_{i+\frac{1}{2}} = \sqrt{a^n_i a^n_{i+1}}.$$

The mach numbers are approximated using

$$M^n_i = \frac{u^n_i}{a^n_{i+\frac{1}{2}}} \quad \text{and} \quad M^n_{i+1} = \frac{u^n_{i+1}}{a^n_{i+\frac{1}{2}}}$$

and the approximation of the pressure terms is

$$\mathbf{P}^n_{i+\frac{1}{2}} = \mathcal{P}^+(M_i)\mathbf{P}^n_i + \mathcal{P}^-(M_{i+1})\mathbf{P}^n_{i+1},$$

where

$$\mathcal{P}^\pm(M) = \begin{cases} \frac{1}{2}(1 \pm \operatorname{sgn}(M)) & \text{if } |M| \geq 1, \\ \frac{1}{4}(M \pm 1)^2(2 \mp M) \pm \alpha M(M^2 - 1)^2 & \text{otherwise.} \end{cases}$$

We require values of α and β and use the optimal values chosen by Liou [9],

$$\alpha = \frac{3}{16} \quad \text{and} \quad \beta = \frac{1}{8}.$$

So far, the scheme is only first order accurate but we require the scheme to be a high resolution scheme. Thus, we adopt the approach discussed in Liou [9], which is based on the MUSCL [14] approach. We first calculate,

$$\mathbf{w}_L = \mathbf{w}_i^n + \frac{1}{2}\mathbf{\Phi}(\theta_i^n)(\mathbf{w}_i^n - \mathbf{w}_{i-1}^n)$$

and

$$\mathbf{w}_R = \mathbf{w}_{i+1}^n - \frac{1}{2}\mathbf{\Phi}\left(\frac{1}{\theta_{i+1}^n}\right)(\mathbf{w}_{i+2}^n - \mathbf{w}_{i+1}^n),$$

and then use the AUSM+ scheme with $\mathbf{w}_{i+1}^n$ and $\mathbf{w}_i^n$ replaced with $\mathbf{w}_R^n$ and $\mathbf{w}_L^n$, respectively. We use the minmod flux-limiter and

$$\theta_i^n = \frac{\mathbf{w}_{i+1}^n - \mathbf{w}_i^n}{\mathbf{w}_i^n - \mathbf{w}_{i-1}^n}$$

for all i. Note that the primitive variables are used for this first step,

$$\mathbf{w} = \begin{bmatrix} \rho \\ u \\ H \end{bmatrix}.$$

We can now use the three different schemes to obtain a numerical approximation of the Euler equations for the four test cases considered in this paper.

4 Numerical Results

We now use the three high resolution schemes to obtain a numerical approximation of the Euler equations for the different test cases and compare with the exact solution (if available), which is obtained from the NUMERICA library [13]. A Courant number of $\nu = 0.25$ will be used for the AUSM+ scheme whereas the other schemes use $\nu = 0.5$. A spatial step-size of $\Delta x = 0.01$ is also used. All test cases are for a domain of length 1 and with $\gamma = 1.4$.

Unless stated, the basic free flow boundary conditions are used,

$$\mathbf{w}_{-i}^{n+1} = \mathbf{w}_0^n \quad \text{and} \quad \mathbf{w}_{i+I}^{n+1} = \mathbf{w}_I^n$$

for $i = 1, 2$.

If an exact solution is available, the L1 error is calculated,

$$||\mathbf{E}||_1 = \Delta x \sum_{i=0}^{I} |\mathbf{E}_i^N|, \quad \text{where} \quad \mathbf{E} = \mathbf{w}(x,t) - \mathbf{w}_i^n \tag{4.1}$$

for the sum of all variables at $t = 0.25$ s (N is the total number of time steps required to reach this time) for each scheme.

4.1 Shock Tube

The first test case is the Shock Tube problem of Sod [11],

$$\rho(x,0) = \begin{cases} 1 & \text{if } x < 0.5, \\ 0.125 & \text{if } x \geq 0.5, \end{cases} \quad p(x,0) = \begin{cases} 1 & \text{if } x < 0.5, \\ 0.1 & \text{if } x \geq 0.5, \end{cases} \quad \text{and} \quad u(x,0) = 0.$$

Figure 4.1 illustrates the results at $t = 0.25$ s. Here, we can see that all three schemes produced very similar results. However, by looking at the L_1 error (4.1), which is displayed in Table 4.1, we can see that the AUSM+ scheme is the most accurate of the three schemes. The HLLE scheme is less accurate than Roe's scheme due to more diffusion being present and thus, there is more diffusion present near shocks. The AUSM+ scheme produced the least amount of diffusion near shocks thus, resulting in the scheme being the most accurate. However, the AUSM+ scheme requires a smaller CFL number than the other two schemes in order to remain stable. This results in a longer computational run time for the AUSM+ scheme.

Scheme	CFL	$\Delta x = 0.01$	0.001	0.0001
Roe	0.5	0.02236295	0.00266800	0.00036183
HLLE	0.5	0.02586942	0.00316410	0.00047531
AUSM+	0.25	0.01548640	0.00217676	0.00066488

Table 4.1: The L_1 error of the schemes for the Shock Tube Problem at $t = 0.25$ s.

4.2 Modified Shock Tube

The second test case is the modified Shock Tube Problem of Sod (adapted by Toro [12]),

$$(\rho, u, p)(x,0) = \begin{cases} (1, 0.75, 1) & \text{if } x < 0.3, \\ (0.125, 0, 0.1) & \text{if } x \geq 0.3, \end{cases}.$$

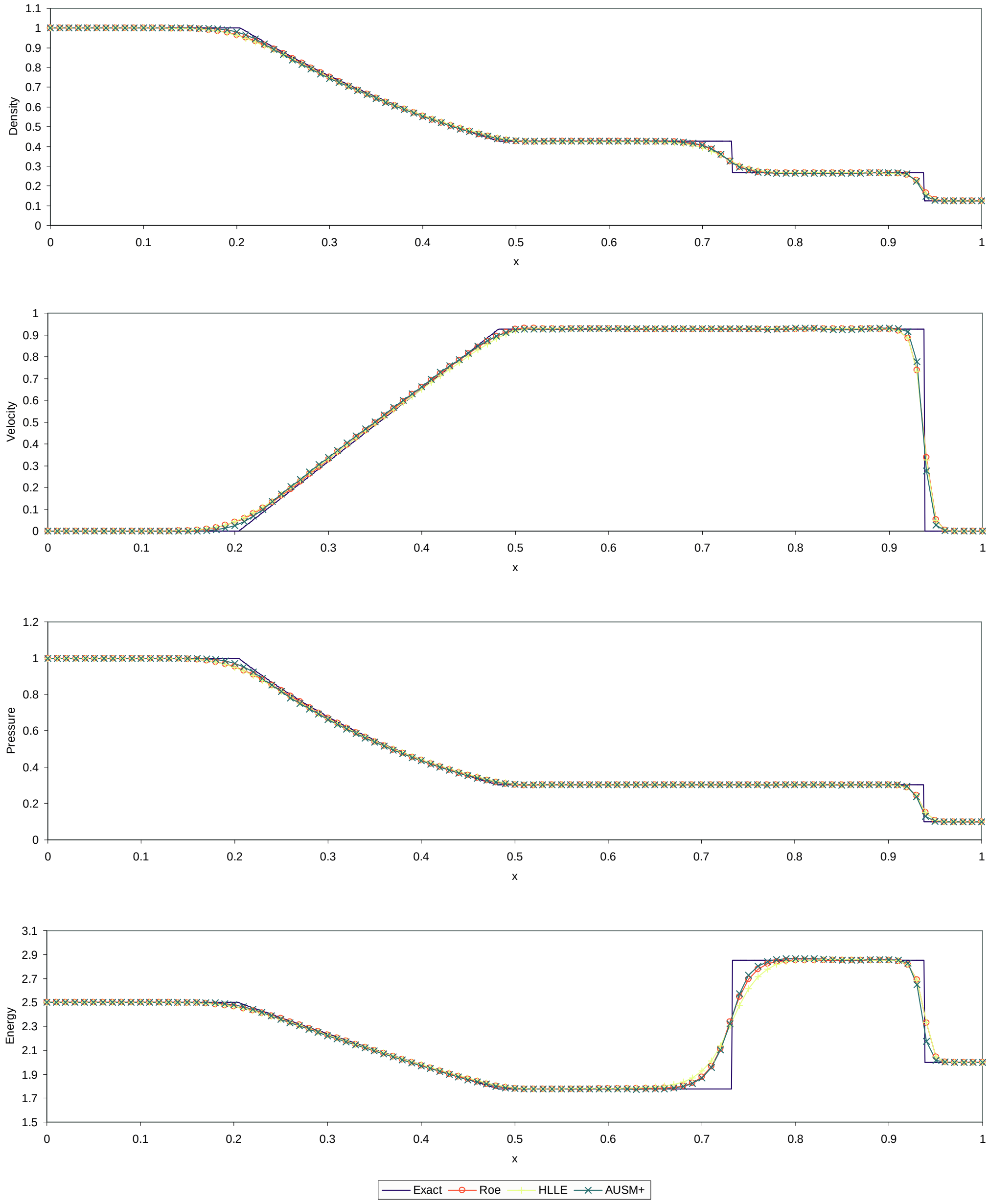

Figure 4.1: Shock Tube Problem at $t = 0.25$.

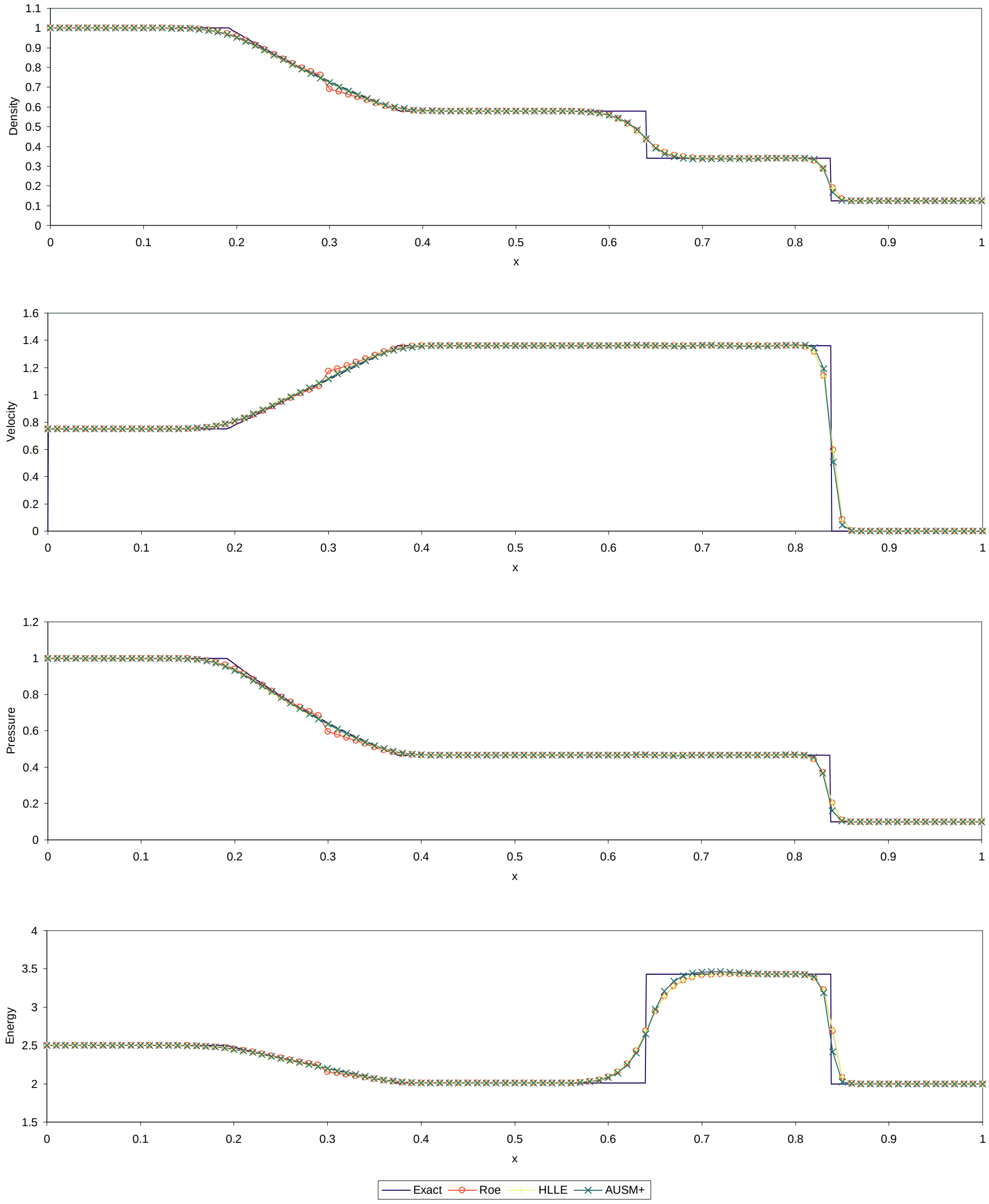

Figure 4.2: Modified Shock Tube Problem at $t = 0.25$.

This test case is designed to test whether the schemes are able to accurately capture rarefaction waves and not produce an entropy glitch. From Figure 4.2, we can see that Roe's scheme has indeed produced an entropy glitch whereas the HLLE and AUSM+ schemes have not. This is due to Roe's scheme being unable to accurately calculate sonic rarefaction waves. There are numerous fixes, e.g. Harten & Hyman [3], for Roe's scheme, but they require tweaking for each test case. The HLLE scheme could be viewed as a fix for Roe's scheme and does not require any tweaking for each test case.

Scheme	CFL	$\Delta x = 0.01$	0.001	0.0001
Roe	0.5	0.02740905	0.00455440	0.00120341
HLLE	0.5	0.02396336	0.00339343	0.00044190
AUSM+	0.25	0.02328236	0.00310239	0.00037837

Table 4.2: The L_1 error of the schemes for the Modified Shock Tube Problem at $t = 0.25$ s.

Unfortunately, the L_1 error (see Table 4.2) of the HLLE scheme is still not as accurate as the AUSM+ scheme. As with the previous test case, the HLLE scheme introduces more dissipation around shocks than the other two schemes. Of course, the HLLE scheme is more accurate than Roe's scheme due to the entropy glitch.

One point worth mentioning here is that if the HLLE scheme is used with $\Phi = 1$ then the scheme reverts to the Lax-Wendroff scheme. Since the Roe average values are used, the scheme produces an entropy glitch in exactly the same manner that Roe's scheme does. However, since near shocks the HLLE scheme is close to first order accurate this is not a concern and an entropy glitch should not form (as can be seen from the results).

4.3 123 Problem

Our third test case is the 123 Problem of Einfeldt *et al.* [1],

$$\rho(x,0) = 1 \quad p(x,0) = 0.4 \quad \text{and} \quad u(x,0) = \begin{cases} -2 & \text{if } x < 0.5, \\ 2 & \text{if } x \geq 0.5. \end{cases}$$

From Figure 4.3, we can see that the HLLE and AUSM+ schemes were the only two which actually produced results. The Roe scheme became unstable almost immediately. Roe's scheme solves the linearized Euler equations, but Einfeldt *et al.* [1] discovered that if

$$\frac{4\gamma\rho e}{3\gamma - 1} - (\rho u)^2 > 0 \quad \text{and} \quad (\gamma - 1)\rho e - (\rho u)^2 \leq 0,$$

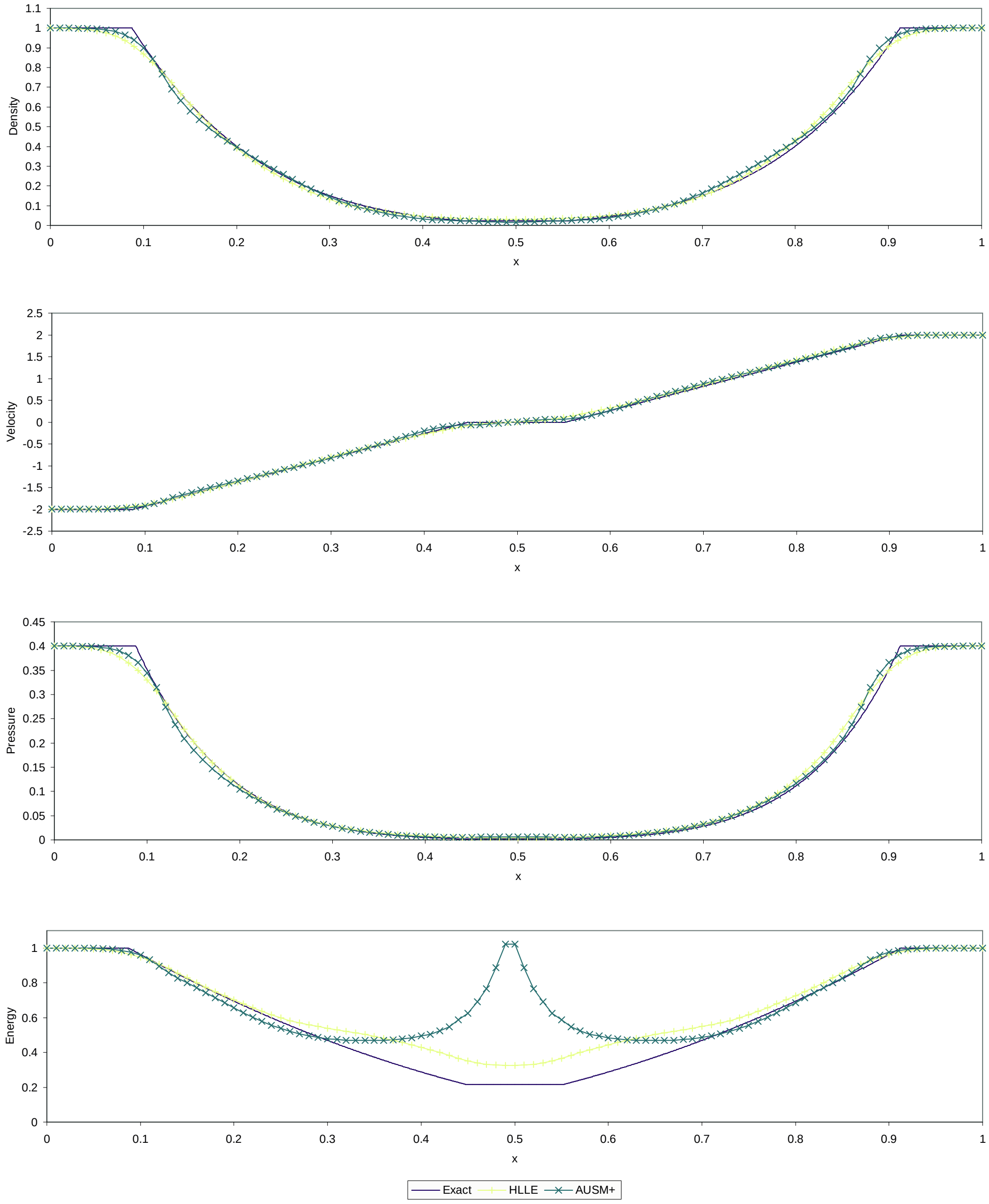

Figure 4.3: 123 Problem at $t = 0.15$.

then the problem is not linearizable. This is due to the data producing a negative density or pressure in the linearized form, but a solution does exist. Since the 123 problem lies in this realm, the problem is not linearizable and thus, Roe's scheme becomes unstable. The HLLE scheme overcomes this problem by adding numerical diffusion to the approximation of the eigenvalues in an attempt to stabilise the scheme. Thus, the failure of Roe's scheme can be viewed as an inaccurate approximation of the physical signal velocities, see Einfeldt *et al.* [1] for more information.

Although the AUSM+ scheme has produced results, the scheme is highly sensitive to this test case and as the mesh is refined, a smaller CFL number is required in order to remain stable and eventually ends up being impractical due to long computational run times. This is illustrated in the calculation of the specific internal energy,

$$e = \frac{p}{(\gamma - 1)\rho},$$

which for this test case can amplify small errors in the other variables. Notice that the HLLE scheme is considerably more accurate than the AUSM+ scheme for the specific internal energy.

4.4 Blast Wave Problem

The final test case is the Blast Wave Problem of Woodward & Colella [15],

$$\rho(x,0) = 1, \quad p(x,0) = \begin{cases} 1000 & \text{if } 0 < x < 0.1, \\ 0.1 & \text{if } 0.1 < x < 0.9, \\ 100 & \text{if } 0.9 < x < 1, \end{cases} \quad \text{and} \quad u(x,0) = 0.$$

For this test case, walls are present at either side of the domain thus, we use the boundary conditions

$$(\rho,p)^{n+1}_{-i} = (\rho,p)^n_{i-1}, \quad u^{n+1}_{-i} = -u^n_{i-1}, \quad (\rho,p)^{n+1}_{I+i} = (\rho,p)^n_{I-i+1} \quad \text{and} \quad u^{n+1}_{I+i} = -u^n_{I-i+1}.$$

From Figure 4.4, we can see that the Roe and HLLE scheme produced similar results. However, the AUSM+ scheme became unstable almost immediately using a CFL = 0.5, but remained stable when a CFL = 0.05 was used (results illustrated).

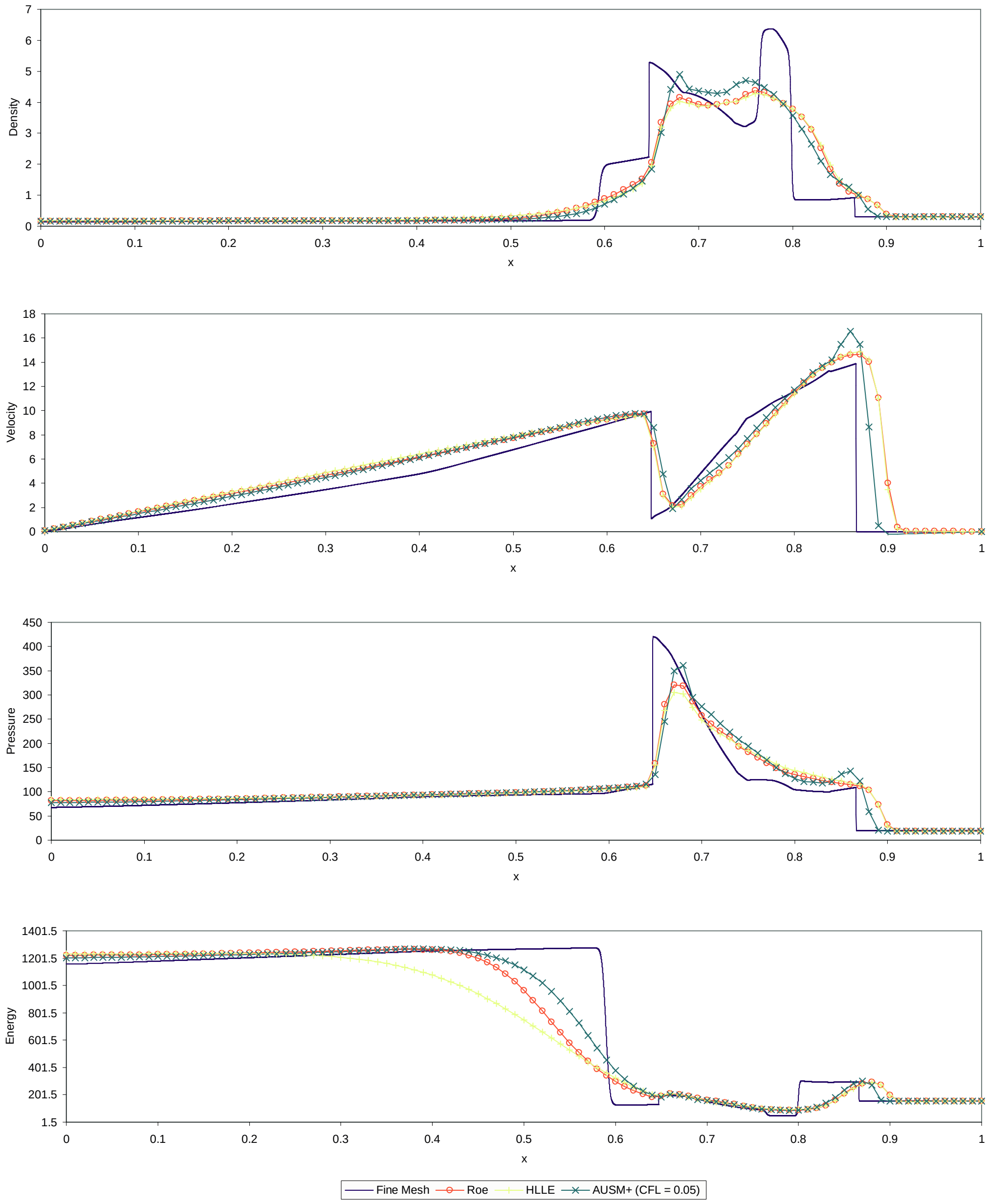

Figure 4.4: Blast Wave Problem at $t = 0.038$.

5 Conclusion

In this paper, we have presented three high resolution schemes and applied them to approximate the Euler equations. Four test cases were used to test each numerical scheme in order to determine their strengths and weaknesses. We illustrated that Roe's scheme suffered from an entropy glitch and was unable to approximate the 123 problem due to the linearization. The HLLE scheme was a lot more robust and could accurate approximate all test cases, but suffered more from numerical diffusion near shocks. The AUSM+ scheme also produced very promising results and did not create and entropy glitch. However, the AUSM+ scheme is very sensitive to the CFL number and requires a smaller CFL number (0.5) than the other schemes (0.8). Moreover, as the mesh is reduced, an even smaller CFL number is required to ensure no spurious oscillation occur in the numerical results. For the blast wave test case, it required a very small CFL number in order for the scheme to remain stable.

Each scheme has certain test cases where it produced better results than the others, but the HLLE was the only scheme which could accurately approximate all four test cases. Thus, overall the HLLE scheme appears to be the most robust out of the three schemes, but suffers from more diffusion than Roe's scheme.

References

[1] B. Einfeldt, C.D. Munz, P.L. Roe & B. Sjogreen, On Godunov-Type Methods Near Low Densities, *J. Comput. Phys.* **92**,273-295 (1991).

[2] A. Harten, P.D. Lax & B. Van Leer, On Upstream Differencing and Godunov-Type Schemes for Hyperbolic Conservation Laws, *SIAM Rev.* **Vol. 25 No.1**, 35 -61 (1983).

[3] A. Harten & J.M. Hyman, Self-Adjusting Grid Methods for One-Dimensional Hyperbolic Conservation Laws, *J. Comput. Phys.* **50**, 235 - 269 (1983).

[4] M.E. Hubbard & P. Garcia-Navarro, Flux Difference Splitting and the Balancing of Source Terms and Flux Gradients, *Numerical Analysis Report* **3/99**, *University of Reading* (1999).

[5] J. Hudson, Numerical Techniques for Morphodynamic Modelling, PhD Thesis, *University of Reading*, October 2001. A colour postscript version of this thesis can be obtained at www.rdg.ac.uk/maths.

[6] Guang-Shan Jiang & Chi-Wang Shu, Efficient Implementation of Weighted ENO Scheme, *J. Comput. Phys.* **126**, 202 - 228 (1996).

[7] R. J. LeVeque, *Finite Volume Methods for Hyperbolic Problems*, Cambridge Tezts In Applied Mathematics, ISBN 0 521 00924 3 (2002).

[8] M.S. Liou & C.J. Steffen, A New Flux Splitting Scheme, *J. Comput. Phys.* **107**, 23 - 39 (1993).

[9] M.S. Liou, A Sequel to AUSM: AUSM+, *J. Comput. Phys.* **129**, 364 - 382 (1996).

[10] P.L. Roe, Approximate Riemann Solvers, Parameter Vectors and Difference Schemes, *J. Comput. Phys.* **43**, 357 - 372 (1981).

[11] G.A. Sod, A Survey of Several Finite Difference Methods for Systems of Nonlinear Hyperbolic Conservation Laws, *J. Comput. Phys.* **27**, 1 - 31 (1978).

[12] E.F. Toro, *Riemann Solvers and Numerical Methods for Fluid Dynamics 2nd Edn*, Springer (1999).

[13] E.F. Toro, *NUMERICA, a Library of Source Codes for Teaching, Research and Applications*, Numeritek Limited (1999).

[14] B. van Leer, Towards the ultimate conservative difference scheme II. Monotonicity and conservation combined in a second order scheme, *J. Comput. phys.* **14**, 361 - 370 (1974).

[15] P.R. Woodward & P. Colella, The Numerical Simulation of Two-Dimensional Fluid Flow With Strong Shocks, *J. Comput. Phys.* **54**,115-173 (1984).

[16] H.C. Yee, Upwind and Symmetirc Shock-Capturing Scheme, *MASA Technical Memorandum* **89464**, (1987).